Editors' Suggestion

Geometric representation of higher-order optical modes

Claire Cisowski
School of Physics and Astronomy, University of Glasgow, Scotland, Glasgow G12 8QQ, United Kingdom

(Received 25 February 2026; accepted 3 June 2026; published 26 June 2026)

An octant representation of higher-order optical modes that includes Laguerre-Gaussian and Hermite-Gaussian modes is presented. The octant picture captures the high-dimensional nature of three-state optical systems and beyond, with standard Poincaré spheres for orbital angular momentum forming subspaces of the entire state space. This representation enables intuitive manipulation of both classical modes and optical qudits and provides a framework for extending Berry phases and topological invariants to high dimensions.

DOI: 10.1103/gf21-tgcm

I. INTRODUCTION

The ability to form mental pictures of physical systems has shaped the history of physics for centuries, with two prominent examples being the Bloch sphere representation of qubits in quantum mechanics [1] and the Poincaré sphere representation of fully polarized light in optics [2]. Recently, the exploration of structured light modes, including Hermite-Gaussian (HG) modes HG_{nm} of indices n and m and Laguerre-Gaussian (LG) modes LG_p^ℓ of radial index p and azimuthal index ℓ, has motivated the development of a geometric toolkit for spatial light. Poincaré sphere analogs have been introduced to describe first-order modes [3], with the mode order being defined as $N = n + m = 2p + |\ell|$, and to represent vector vortex modes in Ref. [4]. By accessing large Hilbert spaces, higher-order spatial modes ($N \geqslant 1$) have emerged as a promising resource for high-dimensional quantum communication [5]. However, visualizing their state spaces is challenging; spheres are no longer sufficient to describe the entire state space, and hyperspheres must be used instead [6]. It is possible to explore subspaces using Poincaré sphere analogs and SU(2) Lie algebra [7], but capturing the topological properties of the entire state space is valuable for studying geometric phases of light in high dimensions [8], holonomic computational gates, and minimal length paths for quantum communication applications [9,10].

In this work, it is shown that the state space of higher-order optical modes can be conveniently visualized as the positive octant of a sphere spanned by a torus. The entire space is covered, except for one two-dimensional subspace where the parametrization is ill defined. The case of second-order modes is taken as a representative example. In contrast to Majorana's stellar representation [11], the strength of which lies in the identification of symmetries in high-dimensional systems, the octant picture directly encodes relative amplitudes and phase between the three base states within its coordinates [6]. Octant coordinates are well adapted to the Fubini-Study metric [6], providing a natural way to measure transition probabilities, distinguishability, and quantum information [12].

II. THE OCTANT REPRESENTATION

The octant representation provides a natural generalization of the Poincaré sphere parametrization. The geometry of two-state systems and their relation to Poincaré spheres, identified as the complex projective space $\mathbb{C}P^1$, is reviewed in the Appendix. Second-order optical modes form a three-state system, written in the formalism of quantum mechanics as $|\psi\rangle = (\psi_1, \psi_2, \psi_3)^T$, with ψ_i denoting complex mode amplitudes. Normalization $|\psi_1^2| + |\psi_2|^2 + |\psi_3|^2 = 1$ reduces the number of parameters needed to describe the system from six real numbers to five, defining a hypersphere S^5. The space of pure states emerges by fixing an overall phase under the equivalence relation $|\Psi\rangle \equiv \lambda\,|\Psi\rangle$ where $\lambda = e^{i\delta}$ is any nonzero complex number. It corresponds to the complex projective space $\mathbb{C}P^2 = S^5/U(1)$. Four independent parameters are therefore needed to parametrize the state space of second-order optical modes. The octant representation introduces four local angle type variables, $(\theta, \phi, \chi_1, \chi_2)$, to parametrize $\mathbb{C}P^2$ [13]. The angles $0 \leqslant \chi_{1,2} < 2\pi$ encode relative phase information. Choosing the third component as the phase reference,

$$|\psi\rangle = e^{i\delta}(n_1 e^{i\chi_1}\,|\psi_1\rangle + n_2 e^{i\chi_2}\,|\psi_2\rangle + n_3\,|\psi_3\rangle), \qquad (1)$$

with $\chi_1 = \arg(\psi_1) - \arg(\psi_3)$, $\chi_2 = \arg(\psi_2) - \arg(\psi_3)$. The real numbers $n_i \geqslant 0$ specify the relative magnitudes of the three components. For normalized states, $n_1^2 + n_2^2 + n_3^2 = 1$, establishing a one-to-one correspondence with points on the positive octant of a sphere (S^2). It follows that the magnitude of the base states can be parametrized by two spherical angles, (θ, ϕ), with their range restricted to $0 \leqslant \theta < \pi/2$ and $0 \leqslant \phi \leqslant \pi/2$ to ensure that only the positive octant of the unit sphere is represented. Combining the amplitude and phase variables,

$$|\psi\rangle = e^{i\delta}(\sin\theta\cos\phi\, e^{i\chi_1}\,|\psi_1\rangle + \sin\theta\sin\phi\, e^{i\chi_2}\,|\psi_2\rangle + \cos\theta\,|\psi_3\rangle). \qquad (2)$$

Published by the American Physical Society under the terms of the Creative Commons Attribution 4.0 International license. Further distribution of this work must maintain attribution to the author(s) and the published article's title, journal citation, and DOI.

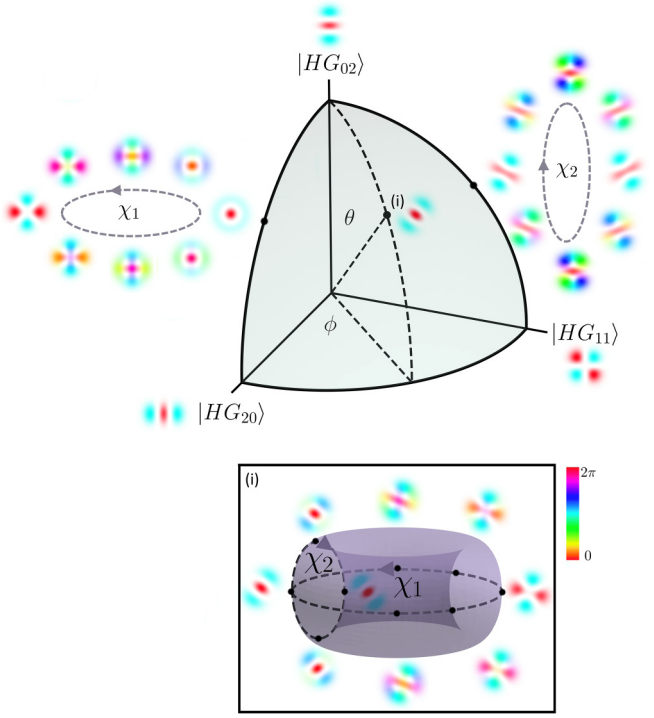


FIG. 1. Octant representation of second-order HG modes. Intensity modulated phase distributions are provided for a set of states. The inset shows the torus structure above (i).

The parametrization breaks down at $\psi_3 = 0$ where relative phases become undefined. The locus $\psi_3 = 0$ is a coordinate singularity defining a sphere, generalizing pointlike singularities in two-state systems [14]. Just as two coordinate charts are needed to cover $\mathbb{C}P^1$, three charts are required to fully cover $\mathbb{C}P^2$ [14]. Equation (2) holds for any three orthonormal bases $\{|\psi_1\rangle, |\psi_2\rangle, |\psi_3\rangle\}$. In each such basis, points on the octant surface specify the weighting between all three base states' contributions, the edges of the octant correspond to a two-state superposition, and its corners identify base states. Allowing χ_1 and χ_2 to vary from 0 to 2π generates a torus keeping track of relative phases above each point on the octant. This torus collapses to a circle on the edges and to a point at the corners where χ_1 and/or χ_2 become undefined. This is readily illustrated with standard second-order structured light modes.

III. HERMITE GAUSSIAN BASIS

In the basis of HG modes, Eq. (2) becomes

$$|\psi\rangle = e^{i\delta}(\sin\theta\cos\phi\, e^{i\chi_1}|\mathrm{HG}_{20}\rangle + \sin\theta\sin\phi\, e^{i\chi_2}|\mathrm{HG}_{11}\rangle + \cos\theta\,|\mathrm{HG}_{02}\rangle). \quad (3)$$

Figure 1 shows the octant representation of HG modes corresponding to Eq. (3). The corners identify the base modes HG_{20}, HG_{11}, and HG_{02}. Along the left edge, states are superpositions of HG_{02} and HG_{20} with χ_2 undefined. The right edge of the octant contains superpositions of HG_{02} and HG_{11} modes with χ_1 undefined. Each edge forms a subspace of $\mathbb{C}P^2$ and can be mapped onto a modal Poincaré sphere by taking the states at the two corners as the poles and identifying the midpoint state and its phase variations as points spanning the equator. The parametrization breaks down where the amplitude of HG_{02} vanishes in Eq. (3), turning the modal sphere of HG_{20} and HG_{11} into a coordinate singularity. It is worth noting that these subspaces stand out due to a choice of basis and, as such, carry no special significance over modal spheres available in an alternative basis from a topological point of view. Coordinate singularities will correspond to different two-dimensional subspaces depending on the choice of basis and phase reference but cannot be removed.

The octant representation clearly illustrates the action of general mode-preserving converters in the HG basis. Building on the formalism of O'Neil and Courtial [15], the SU(3) transformation matrix of a $N = 2$ mode converter, also known as the α converter, can be expressed as

$$C_{\mathrm{HG}}(\alpha) = e^{i2\alpha}\begin{pmatrix} e^{-i2\alpha} & 0 & 0 \\ 0 & e^{-i\alpha} & 0 \\ 0 & 0 & 1 \end{pmatrix}, \quad (4)$$

in the HG basis, where the overall phase factor $e^{-i2\alpha}$ can be discarded. The relative mode amplitudes are not affected by $C_{\mathrm{HG}}(\alpha)$; the (θ, ϕ) coordinates are unchanged, and the state remains at its position on the surface of the octant. Its position on the torus, however, varies. This is made explicit by identifying $\chi_1 = -2\alpha$ and $\chi_2 = -\alpha$. Experimentally, the α converter is typically realized using a pair of cylindrical lenses [16], with the $\alpha = \pi$ and $\pi/2$ configurations being the most commonly employed. The π converter transforms a mode with orbital angular momentum $-\ell$ to one with $-\ell$ and corresponds to an image reflection. In the octant picture, the π converter takes a state to the opposite side of the circle formed by χ_2 as $\chi_1 = -2\pi$ and $\chi_2 = -\pi$. This can be seen in Fig. 1 where the mirror image of the state ($\theta = \pi/4, \phi = \pi/2, \chi_1 =$ undefined, $\chi_2 = 0$) lies at the opposite side of the χ_2 circle. The $\pi/2$ converter can transform a mode with no orbital angular momentum into one possessing it [16]. In the octant representation, the trajectory induced on the torus is given by $\chi_1 = -\pi$ and $\chi_2 = -\pi/2$.

In addition to mode converters, image rotators constitute another important class of transformations for HG and LG modes. The action of a mode rotator matrix of rotation angle Δ is given by [15]

$$R_{\mathrm{HG}}(\Delta) = \begin{pmatrix} \cos^2(\Delta) & \frac{\sin(2\Delta)}{\sqrt{2}} & \sin^2\Delta \\ -\frac{\sin(2\Delta)}{\sqrt{2}} & \cos(2\Delta) & \frac{\sin(2\Delta)}{\sqrt{2}} \\ \sin^2(\Delta) & -\frac{\sin(2\Delta)}{\sqrt{2}} & \cos^2(\Delta) \end{pmatrix}. \quad (5)$$

In the HG basis, a rotation will therefore mix the relative mode amplitudes, forming intricate paths on the octant involving a change in all parameters. For a 45° rotation, Eq. (5) simplifies to

$$R_{\mathrm{HG}}(\Delta = 45^\circ) = \begin{pmatrix} \frac{1}{2} & \frac{1}{\sqrt{2}} & \frac{1}{2} \\ -\frac{1}{\sqrt{2}} & 0 & \frac{1}{\sqrt{2}} \\ \frac{1}{2} & -\frac{1}{\sqrt{2}} & \frac{1}{2} \end{pmatrix}. \quad (6)$$

A 45° rotation takes the HG_{02} mode to the coordinate $(\theta = \pi/3, \phi = \arctan(\sqrt{2}), \chi_1 = 0, \chi_2 = 0)$ as $\mathrm{HG}_{02}(\Delta =$

$45^\circ) = \frac{1}{2}|\mathrm{HG}_{20}\rangle + \frac{1}{\sqrt{2}}|\mathrm{HG}_{11}\rangle + \frac{1}{2}|\mathrm{HG}_{02}\rangle)$. The angular coordinate $(\theta = \pi/3, \phi = \arctan(\sqrt{2}))$ is remarkable in that the torus above it contains $\mathrm{HG}_{20}(\Delta = 45^\circ)$, of phase angles $(\chi_1 = 0, \chi_2 = \pi)$, obtained from a $\alpha = \pi$ conversion as well as $\mathbf{LG}_0^{\pm 2}$ modes obtained from an $\alpha = \pm\pi/2$ conversion, for which $(\chi_1 = -\pi, \chi_2 = \pm\pi/2)$. $\mathrm{HG}_{11}(\Delta = 45^\circ)$ modes are located elsewhere on the octant, at $(\theta = \pi/4, \phi = 0, \chi_1 = -\pi, \chi_2 = \text{undefined})$. The LG_1^0 mode, obtained by $\alpha = \pi/2$ conversion of $\mathrm{HG}_{11}(\Delta = 45^\circ)$, lies on the associated torus with $(\chi_1 = 0, \chi_2 = \text{undefined})$ and $|\mathrm{LG}_1^0\rangle = \frac{1}{\sqrt{2}}|\mathrm{HG}_{20}\rangle + \frac{1}{\sqrt{2}}|\mathrm{HG}_{02}\rangle$.

IV. LAGUERRE GAUSSIAN BASIS

The LG basis provides a more natural setting for describing the action of image rotators. In $\mathbb{C}P^2$, a change of basis is mediated by a SU(3) transformation. For HG and LG modes, basis changes are implemented via [15]

$$B_{\mathrm{HG}\longrightarrow\mathrm{LG}} = \begin{pmatrix} \frac{1}{2} & -\frac{i}{\sqrt{2}} & -\frac{1}{2} \\ \frac{1}{\sqrt{2}} & 0 & \frac{1}{\sqrt{2}} \\ \frac{1}{2} & \frac{i}{\sqrt{2}} & -\frac{1}{2} \end{pmatrix}, \tag{7}$$

$$B_{\mathrm{LG}\longrightarrow\mathrm{HG}} = \begin{pmatrix} \frac{1}{2} & \frac{1}{\sqrt{2}} & \frac{1}{2} \\ \frac{i}{\sqrt{2}} & 0 & -\frac{i}{\sqrt{2}} \\ -\frac{1}{2} & \frac{1}{\sqrt{2}} & -\frac{1}{2} \end{pmatrix}, \tag{8}$$

where $B_{\mathrm{HG}\longrightarrow\mathrm{LG}} = B^{\dagger}_{\mathrm{LG}\longrightarrow\mathrm{HG}}$. In the LG basis, Eq. (2) becomes

$$|\psi\rangle = e^{i\delta}\big(\sin\theta\cos\phi\, e^{i\chi_1}\,|\mathrm{LG}_0^2\rangle + \sin\theta\sin\phi\, e^{i\chi_2}\,|\mathrm{LG}_1^0\rangle + \cos\theta\,|\mathrm{LG}_0^{-2}\rangle\big). \tag{9}$$

Figure 2 shows the octant representation of second-order LG modes. The edges can be mapped onto Poincaré spheres of orbital angular momentum. The right edge defines superpositions of LG_1^0 and LG_0^{-2} modes, whereas the left edge corresponds to superpositions of LG_0^2 and LG_0^{-2} modes, such as the one presented in Ref. [17]. It is important to note that, unlike the sphere of first-order modes, the states at the equator of the sphere obtained by taking $\mathrm{LG}_0^{\pm 2}$ as the poles cannot simply be obtained through the action of a cylindrical lens mode converter.

The octant representation brings insights into optical vortex dynamics by mapping smooth transitions between different weighted superpositions of orbital angular momentum eigenmodes. Figure 3 shows how the phase profile on the octant edges evolves when the relative weighting between the two modes is varied. This could be accomplished, for instance, in an interferometric setup or directly on an amplitude mask. Handedness reversal occurs along the left edge $(\phi = 0)$, mediated by a state carrying an average of zero orbital angular momentum. The right edge $(\phi = \pi/2)$ illustrates the transition from a beam carrying an orbital angular momentum $\ell = +2$ to one with $\ell = 0$, evidencing the splitting of the vortex into two phase singularities of topological charge $\ell = +1$, which are subsequently annihilated by two vortices

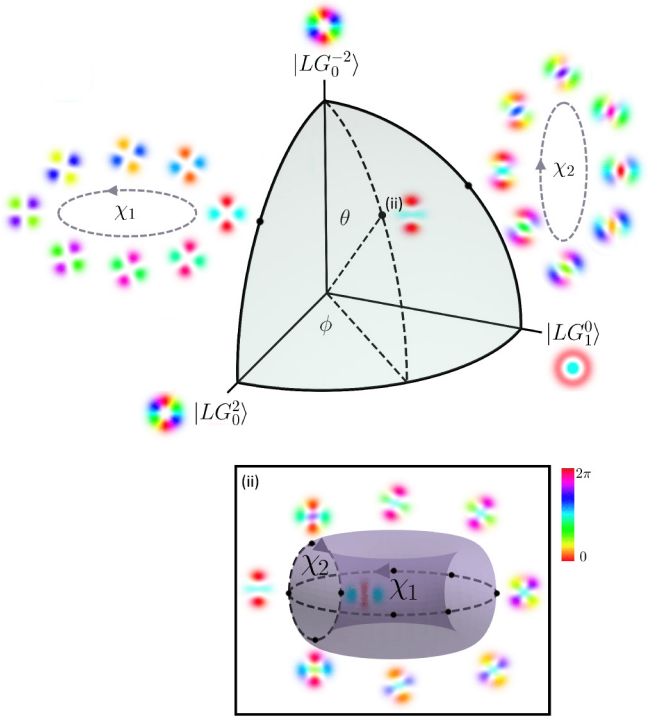


FIG. 2. Octant representation of second-order LG modes. Intensity modulated phase distributions are provided for a set of states. The inset shows the torus structure above (ii).

of opposite charge migrating from spatial infinity. Two mechanisms are therefore highlighted, complementing prior studies dedicated to smooth vortex transformations [18].

In the LG basis, the SU(3) mode rotator matrix is [15]

$$R_{\mathrm{LG}}(\Delta) = e^{-i2\Delta}\begin{pmatrix} e^{i4\Delta} & 0 & 0 \\ 0 & e^{i2\Delta} & 0 \\ 0 & 0 & 1 \end{pmatrix}, \tag{10}$$

where Δ is the rotation angle. Equation (10) confines the state to the torus, without changing its angular position on the octant surface, with $\chi_1 = 4\Delta$ and $\chi_2 = 2\Delta$. A 45° rotation $(\Delta = \pi/4)$ will therefore impose a coordinate change of $\chi_1 = \pi$ and $\chi_2 = \pi/2$, which can clearly be seen in Fig. 2 where the point $(\theta = \pi/4, \phi = 0, \chi_1 = 0, \chi_2 = \text{undefined})$ is taken to the opposite side of the χ_1 circle and for the point $(\theta = \pi/4, \phi = \pi/2, \chi_1 = \text{undefined}, \chi_2 = 0)$ which travels by a quarter of a circle. α-mode converters, on the other

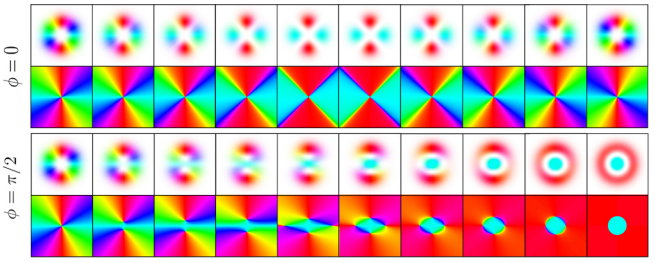


FIG. 3. Phase profile of second-order LG modes, with and without intensity modulation, for increasing θ and fixed ϕ (in all cases $\chi_1 = \chi_2 = 0$).

hand, produce intricate paths in the LG basis, mixing the mode amplitudes and varying relative phases altogether. The α-converter matrix, in the LG basis, reads [15]

$$C_{\mathrm{LG}}(\alpha)=\begin{pmatrix}\cos^2(\alpha/2) & -i\frac{\sin\alpha}{\sqrt{2}} & (\cos^2(\alpha/2)-1)\\ -i\frac{\sin\alpha}{\sqrt{2}} & \cos(\alpha) & -i\frac{\sin\alpha}{\sqrt{2}}\\ (\cos^2(\alpha/2)-1) & -i\frac{\sin\alpha}{\sqrt{2}} & \cos^2(\alpha/2)\end{pmatrix}. \tag{11}$$

For $\alpha=\pi/2$, this simplifies to

$$C_{\mathrm{LG}}(\alpha=\pi/2)=\begin{pmatrix}\frac{1}{2} & -\frac{i}{\sqrt{2}} & -\frac{1}{2}\\ -\frac{i}{\sqrt{2}} & 0 & -\frac{i}{\sqrt{2}}\\ \frac{1}{2} & -\frac{i}{\sqrt{2}} & \frac{1}{2}\end{pmatrix}. \tag{12}$$

An $\alpha=\pi/2$ mode converter will transform a LG_0^+2 mode into $\mathrm{HG}_{02}(\Delta=-45^\circ)$ as $\mathrm{LG}_0^2(\alpha=\pi/2)=\frac{1}{2}\mathrm{LG}_0^2-\frac{i}{\sqrt{2}}\mathrm{LG}_1^0-\frac{1}{2}\mathrm{LG}_0^{-2}$. The corresponding point on the octant $[\theta=\pi/3,\phi=\arctan(\sqrt{2})]$ will then contain HG_{02} and HG_{20} modes on the torus above it. Meanwhile, $\mathrm{LG}_1^0(\alpha=\pi/2)=-\frac{i}{\sqrt{2}}\mathrm{LG}_0^2-\frac{i}{\sqrt{2}}\mathrm{LG}_0^{-2}$ corresponds to a rotated HG_{11} mode of coordinate ($\theta=\pi/4,\pi=0,\chi_1=\pi,\chi_2=$ undefined). The angular coordinates $[\theta=\pi/3,\phi=\arctan(\sqrt{2})]$ and $(\theta=\pi/4,\pi=0)$ coincide with the ones identifying fundamental LG modes in the HG basis. This symmetry can be understood by examining the amplitude of the elements of the mode conversion matrices [Eqs. (7) and (8)].

V. HIGHER DIMENSIONS

The octant representation provides a clear picture of the entire state space of second-order optical modes, embedding Poincaré-like modal spheres within a broader framework and revealing the geometric action of mode converters and mode rotators. It also provides a foundation for exploring vortex dynamics in high-order systems. Its generalization to higher dimensions is straightforward. For a mode of order N, the state space $\mathbb{C}P^{N-1}$ can be represented by positive hyperoctant of an $N-1$ sphere spanned by an $N-1$ torus [6]. The states are parametrized both by N phase angles $0\leqslant\chi_i<2\pi$ describing the torus and by local angles $0<\vartheta_i<\pi/2$ describing the geometry of the hyperoctant. Rearranging terms for clarity, Eq. (2) becomes

$$|\psi\rangle=e^{i\delta}(n_0|\psi_1\rangle+n_1e^{i\chi_1}|\psi_2\rangle+\cdots+n_Ne^{i\chi_N}|\psi_{N+1}\rangle), \tag{13}$$

where

$$\begin{aligned}n_0&=\cos\vartheta_1\sin\theta_2\sin\vartheta_3\cdots\sin\vartheta_n,\\ n_1&=\sin\vartheta_1\sin\vartheta_2\sin\vartheta_3\cdots\sin\vartheta_n,\\ n_2&=\cos\vartheta_2\sin\vartheta_3\cdots\sin\vartheta_n,\\ &\vdots\\ n_n&=\cos\vartheta_n.\end{aligned} \tag{14}$$

Information on relative mode amplitudes and phases is therefore elegantly encoded into two complementary geometric structures, the torus and the hyperoctant.

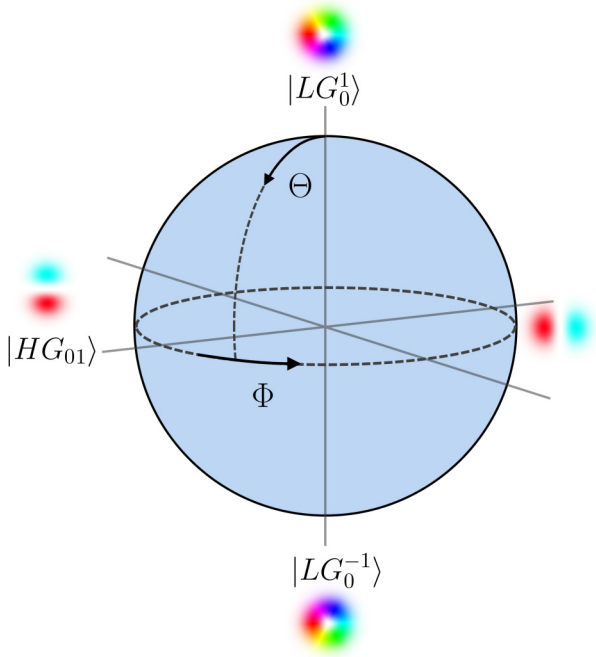


FIG. 4. Sphere of first-order LG modes.

VI. CONCLUSION

The octant representation provides a new tool for studying quantum information theory, phase holonomies, and topological invariants in high-dimensional structured light [17,19,20]. While this paper focuses on scalar modes, a vectorial extension of the octant representation is only a step away, with the potential to highlight new families of vector vortex modes and introduce additional geometric features arising from the nature of the composite system itself. The strength of geometric models is their broad applicability. As a universal description of (pure) high-dimensional state systems, the octant representation can facilitate interdisciplinary knowledge transfer through a shared geometric language. Arguably, one of the most recent examples of such exchange mediated by a geometric model is that of optical skyrmions, which emerged as geometric counterparts of magnetic skyrmions [21,22]. Exploring $\mathbb{C}P^N$ through simple optical transformations could even bring insights into gravitational models [23].

ACKNOWLEDGMENTS

The author is grateful to Professor Brendan Owens for insightful discussions on projective spaces. Financial support from an Early Career Leverhulme fellowship (Grant No. ECF-2023-099) is also acknowledged, in addition to a Lord Kelvin Adam Smith Fellowship (Grant No. LKAS-20318) and an academic returner support fund from the University of Glasgow.

DATA AVAILABILITY

There are no publicly available research data or software supporting this manuscript. Requests for further information or data should be sent to the authors.

APPENDIX: POINCARÉ SPHERE AS A PROJECTIVE SPACE

Fully polarized light and first-order modes are examples of two-state systems described by state vectors $|\psi\rangle = (\psi_1, \psi_2)^T$. $|\psi\rangle$ belongs to a vector space $\mathbb{C}^2$ called Hilbert space. Normalization $\langle\psi|\psi\rangle = 1$ defines a unit hypersphere S^3 in $\mathbb{C}^2$; this space contains global phase information in addition to relative amplitude and phase between the components. Physical states are identified up to a global phase transformation $|\psi\rangle \equiv \lambda\,|\psi\rangle$ where $\lambda = e^{i\delta}$; quotienting out this phase yields the complex projective space $\mathbb{C}P^1 = S^3/U(1)$ as the space of pure states of a two-state system. Importantly, $\mathbb{C}P^1$ is diffeomorphic to the unit sphere S^2. Consequently, the pure state space of a two-state system can be visualized as an ordinary sphere, as exemplified in the Bloch sphere and the Poincaré sphere representations. Two independent parameters are required to characterize (pure) two-state systems, conveniently expressed as the azimuthal and polar angle (Φ, Θ) to encode relative phase and amplitude between the two components such that $|\psi\rangle = (\cos(\Theta/2), e^{i\Phi}\sin(\Theta/2))^T$ with $\psi_1 \neq 0$. Figure 4 illustrates the Poincaré sphere analog for first-order Laguerre Gaussian modes, with $|\mathrm{LG}_0^1\rangle$ and $|\mathrm{LG}_0^-1\rangle$ as base states.

As projective spaces, such Poincaré spheres carry no global phase information. To keep track of this phase, a structure called Hopf fibration can be invoked. This geometric construction consists of a principal U(1) fiber bundle of base space S^2, total space S^3, and fiber U(1). It plays a central role in the identification of geometric phases [8] and has found applications in topological field configurations of light in recent years [24].

[1] F. Bloch, Nuclear induction, Phys. Rev. **70**, 460 (1946).

[2] H. Poincaré, *Théorie Mathématique de la Lumière* (Gabay, Paris, 1892).

[3] M. J. Padgett and J. Courtial, Poincaré-sphere equivalent for light beams containing orbital angular momentum, Opt. Lett. **24**, 430 (1999).

[4] G. Milione, H. I. Sztul, D. A. Nolan, and R. R. Alfano, Higher-order Poincaré sphere, Stokes parameters, and the angular momentum of light, Phys. Rev. Lett. **107**, 053601 (2011).

[5] M. Mirhosseini, O. S. Magaña-Loaiza, M. N. O'Sullivan, B. Rodenburg, M. Malik, M. P. J. Lavery, M. J. Padgett, D. J. Gauthier, and R. W. Boyd, High-dimensional quantum cryptography with twisted light, New J. Phys. **17**, 033033 (2015).

[6] I. Bengtsson and K. Zyczkowski, *Geometry of Quantum States: An Introduction to Quantum Entanglement* (Cambridge University, New York, 2006).

[7] G. F. Calvo, Wigner representation and geometric transformations of optical orbital angular momentum spatial modes, Opt. Lett. **30**, 1207 (2005).

[8] C. Cisowski, J. B. Götte, and S. Franke-Arnold, *Colloquium:* Geometric phases of light: Insights from fiber bundle theory, Rev. Mod. Phys. **94**, 031001 (2022).

[9] M. A. Nielsen, M. R. Dowling, M. Gu, and A. C. Doherty, Quantum computation as geometry, Science **311**, 1133 (2006).

[10] D. C. Brody and L. P. Hughston, Geometric quantum mechanics, J. Geom. Phys. **38**, 19 (2001).

[11] E. Majorana, Atomi orientati in campo magnetico variabile, Il Nuovo Cimento **9**, 43 (1932).

[12] P. Facchi, R. Kulkarni, V. I. Man'ko, G. Marmo, E. C. G. Sudarshan, and F. Ventriglia, Classical and quantum Fisher information in the geometrical formulation of quantum mechanics, Phys. Lett. A **374**, 4801 (2010).

[13] I. Bengtsson, J. Braennlund, and K. Zyczkowski, CP^n, or, entanglement illustrated, Int. J. Mod. Phys. A **17**, 4675 (2002).

[14] M. Nakahara, *Geometry, Topology and Physics*, Graduate Student Series in Physics (Hilger, London, 1990).

[15] A. T. O'Neil and J. Courtial, Mode transformations in terms of the constituent Hermite-Gaussian or Laguerre-Gaussian modes and the variable-phase mode converter, Opt. Commun. **181**, 35 (2000).

[16] M. W. Beijersbergen, L. Allen, H. E. L. O. van der Veen, and J. P. Woerdman, Astigmatic laser mode converters and transfer of orbital angular momentum, Opt. Commun. **96**, 123 (1993).

[17] S. J. M. Habraken and G. Nienhuis, Geometric phases in higher-order transverse optical modes, in *Complex Light and Optical Forces IV*, edited by E. J. Galvez, D. L. Andrews, and J. Glückstad (SPIE, Bellingham, WA, 2010).

[18] G. Molina-Terriza, Vortex transformations and vortex dynamics in optical fields, in *The Angular Momentum of Light*, edited by D. L. Andrews and M. Babiker (Cambridge University, New York, 2012), pp. 31–50.

[19] E. J. Galvez and M. A. O'Connell, Existence and absence of geometric phases due to mode transformations of high-order modes, in *Nanomanipulation with Light*, Proccedings of SPIE Vol. 5736, edited by D. L. Andrews (SPIE, Bellingham, WA, 2005), pp. 166–172.

[20] S. J. van Enk, Geometric phase, transformations of Gaussian light beams and angular momentum transfer, Opt. Commun. **102**, 59 (1993).

[21] C. Cisowski, C. Ross, and S. Franke-Arnold, Building paraxial optical skyrmions using rational maps, Adv. Photonics Res. **4**, 2200350 (2023).

[22] Z. Ye, S. M. Barnett, S. Franke-Arnold, J. B. Götte, A. McWilliam, F. C. Speirits, and C. M. Cisowski, Theory of paraxial optical skyrmions, Proc. R. Soc. A **480**, 20240109 (2024).

[23] G. W. Gibbons and C. N. Pope, $\mathbb{C}\mathrm{P}^2$ as a gravitational instanton, Commun. Math. Phys. **61**, 239 (1978).

[24] D. Sugic, R. Droop, E. Otte, D. Ehrmanntraut, F. Nori, J. Ruostekoski, C. Denz, and M. R. Dennis, Particle-like topologies in light, Nat. Commun. **12**, 6785 (2021).